Research Article | Vol. 8, No. 1 | 1 Jan 2018 | OPTICAL MATERIALS EXPRESS 1

Optical Materials EXPRESS

Intrinsic second harmonic generation from un-poled doped silica multilayered thin films

SEYED HAMED JAFARI,[1] JOSE ANTONIO NOVOA LOPEZ,[1] TAHSEEN HAQUE,[1] JACQUES ALBERT,[1] AND CHRISTOPHER W. SMELSER[1,2,*]

[1]*Department of Electronics, Carleton University, 1125 Colonel By Drive, Ottawa, ON, K1S 5B6, Canada*
[2]*Carleton School of Information Technology, Carleton University, 1125 Colonel By Drive, Ottawa, ON, K1S 5B6, Canada*
**Christopher.Smelser@carleton.ca*

Abstract: Second harmonic light generation (SHG) was observed from as-deposited silica glass thin films suitable for waveguiding, without the need for an inversion symmetry-breaking poling treatment. Thin film stacks of up to 16 layers of alternating 2% phosphorus-doped and undoped silica glass on silica substrates were prepared and probed with a pulsed Nd:YAG laser at 1064 nm. We observed that even though these structures were not poled, they possess a net second order non-linearity with a value of the order of 0.03 pm/V. The SHG increased with the number of layers (total thicknesses between 4 and 9.6 μm have been tested) and also depended on the thickness ratio between the doped and undoped layers. Annealing at 800°C for 4 hours removed the nonlinearity completely.

OCIS codes: (190.4400) Nonlinear optics, materials; (190.4160) Multiharmonic generation; (160.2750) Glass and other amorphous materials.

References and links

1. R. A. Myers, N. Mukherjee, and S. R. J. Brueck, "Large second-order nonlinearity in poled fused silica," Opt. Lett. **16**(22), 1732–1734 (1991).
2. M.-V. Bergot, M. C. Farries, M. E. Fermann, L. Li, L. J. Poyntz-Wright, P. St. J. Russell, and A. Smithson, "Generation of permanent optically induced second-order nonlinearities in optical fibers by poling," Opt. Lett. **13**(7), 592–594 (1988).
3. V. Mizrahi and J. E. Sipe, "Generation of permanent optically induced second-order nonlinearities in optical fibers by poling: comment," Appl. Opt. **28**(11), 1976–1977 (1989).
4. P. G. Kazansky and V. Pruneri, "Electric-field poling of quasi-phase-matched optical fibers," J. Opt. Soc. Am. B **14**, 3170–3179 (1997).
5. C. Corbari, A. V. Gladyshev, L. Lago, M. Ibsen, Y. Hernandez, and P. G. Kazansky, "All-fiber frequency-doubled visible laser," Opt. Lett. **39**(22), 6505–6508 (2014).
6. E. L. Lim, C. Corbari, A. V. Gladyshev, S. U. Alam, M. Ibsen, D. J. Richardson, and G. Kazansky, "Multi-Watt All-Fiber Frequency Doubled Laser," in *Advanced Photonics*, OSA Technical Digest (online) (Optical Society of America, 2014), paper JTu6A.5.
7. O. Tarasenko and W. Margulis, "Electro-optical fiber modulation in a Sagnac interferometer," Opt. Lett. **32**(11), 1356–1358 (2007).
8. T. Fujiwara, D. Wong, Y. Zhao, S. Fleming, S. Poole, and M. Sceats, "Electro-optic modulation in germanosilicate fibre with UV-excited poling," Electron. Lett. **31**(7), 573–575 (1995).
9. S. Fleming and H. An, "Poled glasses and poled fiber devices," J. Ceram. Soc. Jpn. **116**(1358), 1007–1023 (2008).
10. R. H. Stolen and H. W. K. Tom, "Self-organized phase-matched harmonic generation in optical fibers," Opt. Lett. **12**(8), 585–587 (1987).
11. U. Österberg and W. Margulis, "Dye laser pumped by Nd:YAG laser pulses frequency doubled in a glass optical fiber," Opt. Lett. **11**(8), 516–518 (1986).
12. A. R. Camara, J. M. B. Pereira, O. Tarasenko, W. Margulis, and I. C. S. Carvalho, "Optical creation and erasure of the linear electrooptical effect in silica fiber," Opt. Express **23**(14), 18060–18069 (2015).
13. D. Wong, W. Xu, S. Fleming, M. Janos, and K.-M. Lo, "Frozen-in electrical field in thermally poled fibers," Opt. Fib. Tech. **5**(2), 235–241 (1999).
14. P. G. Kazansky and P. St. J. Russel, "Thermally poled glass: frozen-in electric field or oriented dipoles?" Opt. Commun. **110**(5–6), 611–614 (1994).

#308422 https://doi.org/10.1364/OME.8.000001
Journal © 2018 Received 2 Oct 2017; revised 22 Nov 2017; accepted 26 Nov 2017; published 4 Dec 2017

Optical Materials EXPRESS

15. A. Camara, O. Tarasenko, and W. Margulis, "Study of thermally poled fibers with a two-dimensional model," Opt. Express **22**(15), 17700–17715 (2014).
16. T. G. Alley, R. A. Myers, and S. R. J. Brueck, "Space charge dynamics in thermally poled fused silica," J. Non-Cryst. Solids **242**, 165–176 (1998).
17. H. Takebe, P. G. Kazansky, P. St. J. Russell, and K. Morinaga, "Effect of poling conditions on second-harmonic generation in fused silica," Opt. Lett. **21**(7), 468–470 (1996).
18. Y. Quiquempois, A. Kudlinski, and G. Martinelli, "Zero-potential condition in thermally poled silica samples: evidence of a negative electric field outside the depletion layer," J. Opt. Soc. Am. B **22**(3), 598–604 (2005).
19. Y. Luo, A. Biswas, A. Frauenglass, and S. R. J. Brueck, "Large second-harmonic signal in thermally poled lead glass-silica waveguides," Appl. Phys. Lett. **84**, 4935–4937 (2004).
20. J. Fage-Pedersen, R. Jacobsen, and M. Kristensen, "Poled-glass devices: influence of surfaces and interfaces," J. Opt. Soc. Am. B **24**, 1075–1079 (2007).
21. D. Faccio, A. Busacca, D. W. J. Harwood, G. Bonfrate, V. Pruneri, and P. G. Kazansky, "Effect of core-cladding interface on thermal poling of germanosilicate optical waveguides," Opt. Commun. **196**, 187–190 (2001).
22. H. L. An and S. Fleming, "Controlling spatial distribution of thermal poling induced second-order optical nonlinearity with multilayered structures," Appl. Phys. Lett. **101**, 101101 (2012).
23. K. Yadav, C. W. Smelser, S. Jacob, C. Blanchetiere, C. L. Callender, and J. Albert, "Simultaneous Corona Poling of Multiple Glass Layers for Enhanced Effective Second-Order Optical Nonlinearities," Appl. Phys. Lett. **99**, 031109 (2011).
24. K. Yadav, C. L. Callender, C. W. Smelser, C. Ledderhof, C. Blanchetiere, S. Jacob, and J. Albert, "Giant enhancement of the second harmonic generation efficiency in poled multilayered silica glass structures," Opt. Express **19**(27), 26975–26983 (2011).
25. R. W. Boyd, *Nonlinear optics* (Academic press, 2003).
26. Y. R. Shen, "Surface second harmonic generation: a new technique for surface studies," Annu. Rev. Mater. Sci. **16**(1), 69–86 (1986).
27. L. Alloatti, C. Kieninger, A. Froelich, M. Lauermann, T. Frenzel, K. Köhnle, W. Freude, J. Leuthold, M. Wegener, and C. Koos, "Second-order nonlinear optical metamaterials: ABC-type nanolaminates," Appl. Phys. Lett. **107**(12), 121903 (2015).
28. S. Clemmen, A. Hermans, E. Solano, J. Dendooven, K. Koskinen, M. Kauranen, E. Brainis, C. Detavernier, and R. Baets, "Atomic layer deposited second-order nonlinear optical metamaterial for back-end integration with CMOS-compatible nanophotonic circuitry," Opt. Lett. **40**(22), 5371–5374 (2015).
29. A. Hermans, C. Kieninger, K. Koskinen, A. Wickberg, E. Solano, J. Dendooven, M. Kauranen, S. Clemmen, M. Wegener, C. Koos, and R. Baets, "On the determination of $\chi^{(2)}$ in thin films: a comparison of one-beam second-harmonic generation measurement methodologies," Sci. Rep. **7**, 44581 (2017).
30. A. Yariv, Quantum Electronics (2nd ed.) (John Wiley and Sons, New York, 1975).
31. C. T. Sah, H. Sello, and D. A. Tremere, "Diffusion of phosphorus in silicon oxide film," J. Phys. Chem. Solids **11**, 288 (1959).
32. SPECTRAGLASS Limited Unit 2, Inveralmond Close, Inveralmond Industrial Estate, Perth PH1 3TT, *http://www.spectraglass.com/images/pdf/M006%20Quartz%20(JGS2).pdf*.
33. M. Fokine, K. Saito, and A. J. Ikushima, "Thermally induced second-order nonlinearity in silica-based glasses," Appl. Phys. Lett. **87**, 171907 (2005).

1. Introduction

The creation of an efficient second-order optical nonlinearity (SON) over thicknesses of the order of a few microns near the surface of bulk silica glass is possible by thermal poling at a few hundred °C and imposed electric fields of the order of 50 kV/cm [1]. The accepted model for this effect is that of charge migration (from ion impurities in the glass) under the externally imposed electric field, which results in a permanent frozen-in electric field in the glass after cooling. Coupling of the internal DC electric field with the ever present third order nonlinearity of the glass gives rise to a χ^2 coefficient of the order of 1 pm/V. This technique has been widely used over the years to fabricate glass-based optical fiber and waveguide devices for second harmonic generation and electro-optical switching [2–9]. In all cases the effect is too small to be practical unless large interaction lengths are used, which brings additional problems in phase matching and pulse walk-off [4-5,9]. It is therefore desirable to find ways to increase the magnitude of the effective nonlinearity in such glass waveguiding structures in order to reduce their length. Going back to earlier observations of weaker induced second order nonlinearities in glass optical fibers [10–12], and to other forms of poling [2,8], all models used to explain the observed effects are based on some spatial redistribution of charges that break the natural inversion symmetry of the glass [2,13-18]. Further experimental investigations of the distribution of the induced nonlinearity across

Optical Materials EXPRESS

planar and fiber samples also show that when interfaces are present (thin films on substrates, or near the core-cladding boundary of fibers), charge migration is perturbed at these interfaces, and SON peaks associated with the localization of the frozen-in fields appear [19-22]. In two previous publications on this topic, we formulated the hypothesis that a net increase in the effect of these weak SON layers could be obtained by stacking them in such a way that interaction volume between light waves and the nonlinearity increases, either with light going across a sample with a thicker SON region, or in a waveguiding configuration where the optical modes with multi-μm lateral dimensions overlap more completely with the SON. The results showed that the SHG from such stacks does scale with the number of layers, and that the thickness over which the SON is created also increases [23,24]. A maximum enhancement factor of 204X the SHG over a bulk silica sample was reached for a 40 layer stack of 75 nm-thick alternating doped and undoped silica glass layers, for a total thickness of only 3 μm [24].

The current paper investigates whether a similar effect could arise if a stack of unpoled glass layers could show some SON over a significant thickness, due to the replication of the surface SHG effect [25]. This surface effect arises because the inversion symmetry of a bulk glass sample is necessarily broken at its interface with another medium, leading to a molecularly thin SON layer [26]. While surface SHG has been used extensively to probe the properties of surfaces and of adlayers on surfaces there does not appear to have been studies on whether surface SHG could occur in media with multiple parallel interfaces.

However a related phenomenon was recently demonstrated in Alloatti et al. where an "artificial" nonlinear crystal was fabricated by stacking groups of three layers of different transparent centrosymmetric materials (oxides of Hf, Ti, and Al, generically labelled A, B, and C, each with no intrinsic SON) such that the polarizability of the compound material is different in the ABC direction than in the CBA direction [27]. Using atomic layer deposition (ALD) to fabricate their samples, they demonstrated a nonlinear susceptibility of 0.26 pm/V at 800 nm with a "nanolaminate" made up of individual layer thicknesses of the order of 3 nm. This concept was further optimized by Clemmen et al. who used similar material (only replacing Hf by In in the recipe) and 0.7 nm thick individual layers, reaching a value of 5 pm/V for the nonlinear susceptibility, over a total thickness of 50 nm [28-29]. It is likely that the large increase in the nonlinearity came from the reduced thickness, since the lattice spacing of the composite material approaches that of common nonlinear crystal. As noted by these authors, the small thickness (limited by the relatively slow ALD process) implies that these nonlinear layers cannot be realistically considered for waveguide fabrication, but rather as a cladding for waveguides, submicron sized CMOS compatible silicon nitride rib waveguide for instance, where an overlap of 50% between the guided mode and the cladding can be obtained [28]. Our work is completely different because it is based on the inherent asymmetry of the electronic polarizability which occurs automatically at any interface between different materials (leading to surface SHG), multiplied by stacking many such interfaces in such a way that the SHG waves generated from adjacent pairs of interfaces do not cancel.

Here we investigate this different approach with plasma-enhanced chemical vapor deposition (PECVD) of silica glass, a fabrication process compatible with optical waveguide fabrication (and with optical fiber preform fabrication). Also, instead of artificially building a material with broken inversion symmetry, we use only two different materials and hypothesize that the surface SHG effect will occur at all the interfaces between the two types of layers and that an average SON layer extending across the whole stack of layers will be formed. Alternating un-doped and doped silica glass were used with individual thicknesses between 0.2 and 1 μm and total thicknesses up to 9.6 μm. These sizes (and the doping levels we used) are compatible with single mode waveguide core dimensions and thus perfect overlap between the SON and guided mode. According to the theoretical principles explained in [27-28], such dual metamaterials should not break the inversion symmetry (the average

Optical Materials EXPRESS

material polarizability change should cancel between the AB and BA interfaces). However, in the remainder of this paper, it is shown that a significant increase in second harmonic generation (SHG) from such structures was found. The effects of the layer configuration and of thermal post-processing are studied and possible explanations for the unexpected presence of the SON are discussed.

2. Experiment

Thin film multilayer structures consisting of alternating layers of 2 wt% phosphorus-doped and un-doped silica were deposited on a double side polished, 500 μm thick fused silica substrate (made from JGS2 glass, with 150 ppm OH- and 20-40 ppm impurity content) by PECVD at 350°C, and a deposition rate of ~100 nm/minute. No post deposition anneal was performed on the samples. Figure 1 shows the two kinds of samples used for the SHG measurement. Set A samples are composed of equal thickness 500 nm-thick doped and un-doped layers while Set B samples had 1 μm-thick un-doped silica and 200 nm-thick doped silica. For both kinds of samples, 8 and 16 layer structures were fabricated and studied.

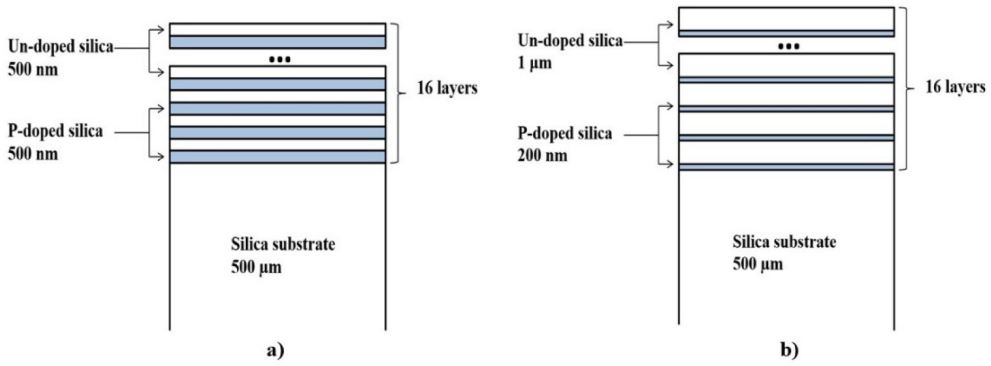

Fig. 1. Multi-layer structures: a) multi-layer structures "A" consisting of alternating 500 nm thick P-doped (2 wt%) and undoped silica layers. b) multi-layer structures "B" consisting of alternating 200 nm thick P-doped (2 wt%) and 1 μm thick undoped silica layers. 8 and 16-layer samples were tested.

The existence of a SON layer in the samples verified by the generation of second harmonic light in a Maker fringe experiment (Fig. 2). The measurement system consists of a diode-pumped solid-state laser (Passat Compiler) operating at 1064 nm with 8 ps pulses at 500 pulses per second, a beam radius of ~1mm and a maximum pulse energy of 2 mJ. The laser was focused with a 150 mm focal length lens onto the samples. The samples were fixed on the axis of a rotation stage and SHG measured as function of the incidence angle. The laser beam was linearly polarized and the polarization could be rotated in the s or p-plane with a Glan-Thompson polarizer. The power incident on the sample could be varied with the use of a half-wave plate prior to the polarizer. A long pass filter placed between down collimating lenses, L1 and L2, was used to eliminate any residual SHG that may be generated within the laser. After the sample the SHG light was selected by a band-pass filter at 532 nm and further separated from the residual 1064 nm pump with a prism. The light was then detected with a Hamamatsu H7827-001 19 mm diameter voltage-type photomultiplier tube sensitive in the 300–650 nm range (blind at 1064 nm), connected to an oscilloscope.

Optical Materials EXPRESS

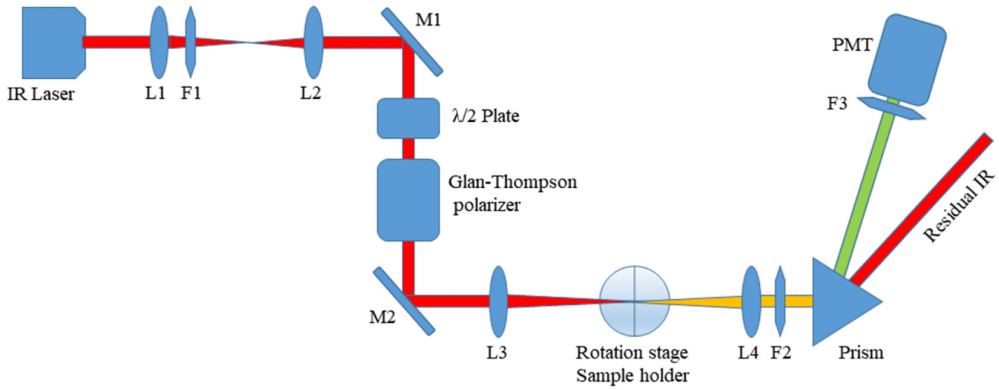

Fig. 2. Maker fringe measurement apparatus consisting of Q-switched Nd:YAG laser at 1.064 µm, down collimating lenses L1: FL 5 cm and L2: FL 2.5 cm, focusing lens L3: FL 15 cm, L4: FL 10 cm lens, F1: Long-pass filter (blocks λ<800 nm), F2: short-pass filter (blocks λ>800 nm), F3: band-pass filter centered on 532 nm, M1 and M2: dielectric mirrors.

3. Experimental results

3.1 Effect of layer structure

The SHG generated by unpoled 8 and 16 layer structures is shown in Fig. 3, with an additional measurement on a bare substrate. All measurements were made in the same conditions, with an average laser power of 21 mW, and p-polarized light. No SHG was observed for s-polarized light.

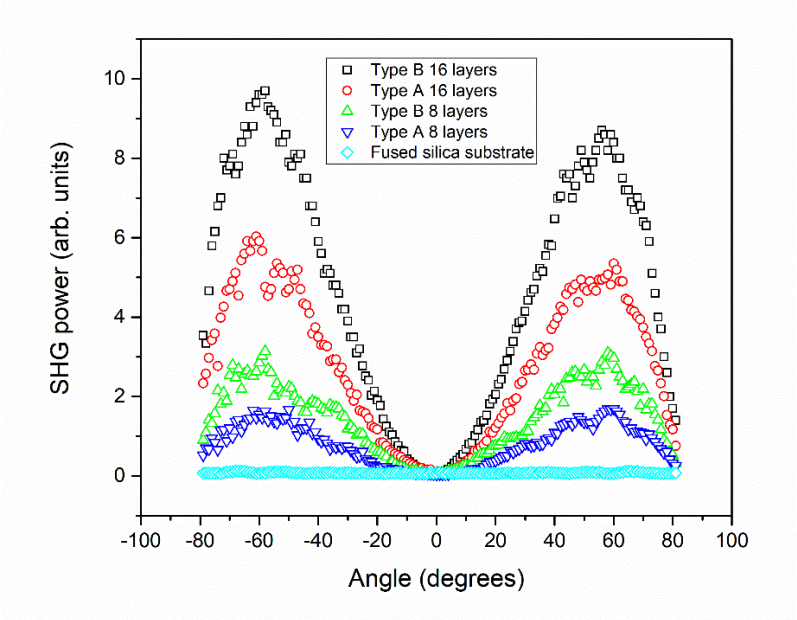

Fig. 3. Measured SHG as a function of incidence angle for 4 samples and a bare substrate (see text for sample descriptions).

Apart from the significant increase in the SHG from the samples with layers compared to the bare substrate, the first observation is that the Maker fringes do not oscillate significantly with angle, indicating that the SON is thinner than the coherence length between the pump and SHG waves. It was verified that the slight asymmetry between the positive and negative

Optical Materials EXPRESS

angles relative to normal is an experimental artefact and not due to anisotropy in the samples. The second finding is that the SHG is larger by 70% for Type B structures relative to Type A and that it increases with the number of layers. In order to help quantify those differences, Fig. 4 shows how the SHG scales between the 8 layer and the 16 layer samples, for Type A and Type B. The ratio of SHG was not smoothed or averaged and is only shown for angles above 30 degrees, where the signal to noise is sufficient to yield reliable values. It turns out that the SHG increases by a factor between 3.2 and 3.5, depending on sample type, when the number of layers is doubled.

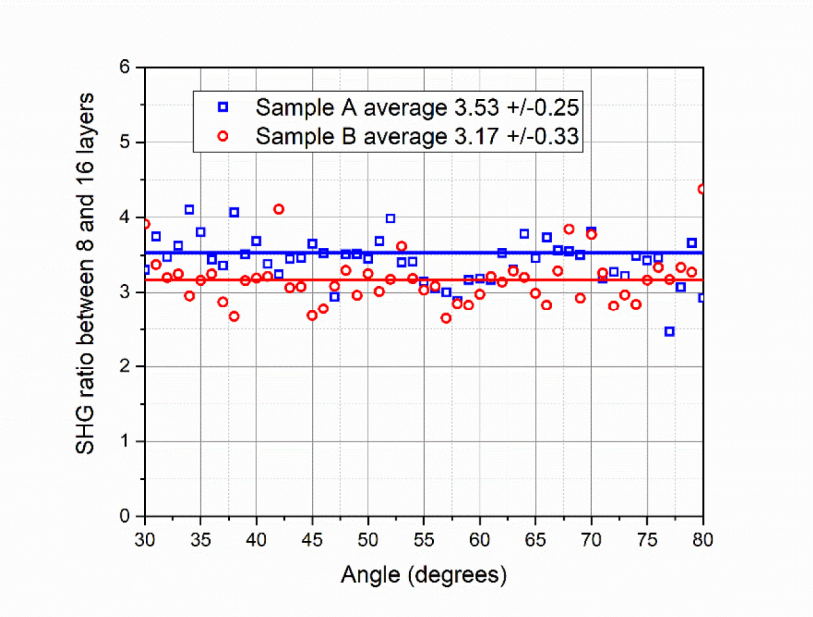

Fig. 4. Ratio of the measured SHG at angles of incidence between 30 and 80 degrees from Fig. 3. Labels "A" and "B" refer to samples with different thickness ratios (see text for details).

According to our hypothesis, an electromagnetic wave at the second harmonic from the pump should be generated at each interface between the layers and as a result the total SHG power should scale quadratically with the number of layers. However, the SHG waves generated from each layer add coherently and the accumulated phase mismatch between the pump and SHG waves prevents this quadratic growth as the thickness increases to values approaching the coherence length. As an estimate of the coherence length l_c in the multilayer stack, we take the values for fused silica according to:

$$l_c = \frac{\lambda}{2(n_{2\omega} - n_{\omega})} \tag{1}$$

where λ is the pump wavelength in vacuum (1064 nm), $n_{2\omega}$ is the refractive index of silica at 532 nm (1.4607), and n_{ω} the index at 1064 nm (1.4497). The coherence length is then 48 µm, i.e. close to 5 times the thickness of our thickest sample, but enough to decrease the SHG by a small amount, which contribute to the smaller than expected ratio of SHG. We used the following simple model for the conversion efficiency η_{SHG} between the pump (P^{ω}) and SHG ($P^{2\omega}$) power (Eq. (16).5-5 from [30]).

Optical Materials EXPRESS

$$P^{2\omega} = 2T\left(\frac{\mu_0}{\epsilon_0}\right)^{3/2}\frac{\omega^2 d^2 L^2}{n^3}\left(\frac{\left(P^{\omega}\right)^2}{A}\right)\frac{\sin^2\left(\frac{\Delta kL}{2}\right)}{\left(\Delta kL/2\right)^2} \quad (2)$$

where T is a factor which includes the effect of all reflections, ω is the pump frequency, *d* the second-order nonlinear coefficient, L the path length in the nonlinear material, A the area of the incident beam on the sample, Δk the phase mismatch (equal to $(2\omega/c)(n_{2\omega}-n_{\omega})$. In Eq. (2) the usual approximation that $\varepsilon_{\omega}\approx\varepsilon_{2\omega}\approx\varepsilon_0 n^2$ was used (these values differ by less than 5% here), and it is assumed that no significant pump depletion occurs (which is certainly the case here). Eq. (2) can be used to explain the observed ratios between 8 and 16 layer samples since the only parameter remaining from ratios of similar experiments on similar material samples is the $\sin^2(\Delta kL/2)$ factor. For type A samples, increasing the thickness from 4 to 8 μm should increase the SHG power by a factor of 3.7, while for the type B samples the expected increase in going from 4.8 to 9.6 μm is 3.6 times, both within the standard deviation of the observed ratios (and with the correct trend, i.e. with a smaller ratio for Type B). This implies that in order to increase the SHG output from these samples in transmission, quasi-phase-matching would be required (i.e. periodic "spacer" layers without nonlinearity). However the goal is to fabricate waveguiding structures from these layers: much longer path lengths are then achievable and quasi-phase-matching can be carried out by periodic erasure of the SON (as in [5]).

In order to investigate the origin of the significant higher SHG observed in Type B samples at thicknesses comparable to Type A samples, annealing and composition studies were carried out.

3.2 Effect of doping

Separate experiments were carried out with samples of the Type B and various concentrations of phosphorus in the doped silica layers. The results, shown in Fig. 5, indicate the somewhat surprising result that the amount of doping has little effect on the formation of the SON in these multilayer structures over the range tested.

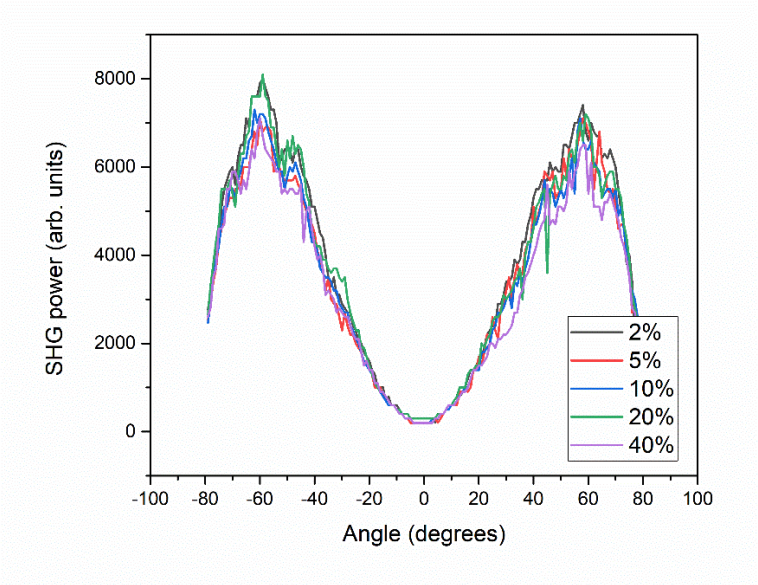

Fig. 5. SHG power as a function of the weight % of phosphorus in samples with 8 layers of Type B.

Optical Materials EXPRESS

3.3 Effect of annealing

A preliminary test was carried out to determine whether the induced SON is stable after annealing at 800°C for 4 hours. The result (not shown) is that annealing completely removed the SHG from a 16-layer sample of Type B. On the other hand, a 5 minute anneal at 300°C yielded no change in SHG. Even at 800°C the diffusion coefficient of phosphorus in silica is $4X10^{-4}$ μm^2/hr, meaning a diffusion length of the order of 0.04 μm over 4 hours [31]. This diffusion length is insufficient to erase the doping contrast since the pure silica layers are between 0.5 and 1 μm thick. Therefore the SON observed here is not due to an alternating material composition as in refs [27-28], and further implies that a ternary structure (three different materials) is not needed. However, the 800 °C annealing temperature is relatively close to the strain point of silica (1120°C) [32]. Since the strain point of doped silica should be somewhat lower, it is likely that some amount of strain relief can occur in our structures at 800°C, thereby supporting the hypothesis that interface strain plays a role in the formation of a SON region in our samples. This strain should be higher in Type B structures because the thicknesses of the stiffer pure silica layers are larger relative to the softer phosphorus doped ones (than in Type A), which would explain the larger SHG observed in these samples. Finally, a strain gradient extending from the top layer surface down towards the substrate surface should be present due to differential expansion during cool down from the PECVD process temperature of 350°C. It is interesting to note that it was demonstrated by Fokine et al. that rapid quenching of bulk silica glass samples results in the formation of a ≈5 μm thick SON region extending from the surface of the samples, and explained by a stress gradient that was responsible for the breaking of the inversion symmetry over this region [33]. They further demonstrated that the SHG was maximum when the heating temperature prior to quenching was 1200 °C (i.e. very near the strain point of silica). In the present case, the simultaneous effects of localized stress at each layer interface and bulk stress gradient is thought to be responsible for both the increased SHG from Type B samples and also the fact that the induced SON does not appear to alternate in sign at doped-undoped and undoped-doped interfaces (which would reduce the SHG if it did).

3.4 Validation of SHG growth

Given that no SHG was expected from unpoled glass, the quadratic behavior of the detected signal was verified to eliminate the possibility of a systematic experimental error. Figure 6 shows how the SHG power at 532 nm scales with the input 1064 nm power. A second-order dependence (illustrated by the pure quadratic fitting function shown) is clearly observed.

Optical Materials EXPRESS

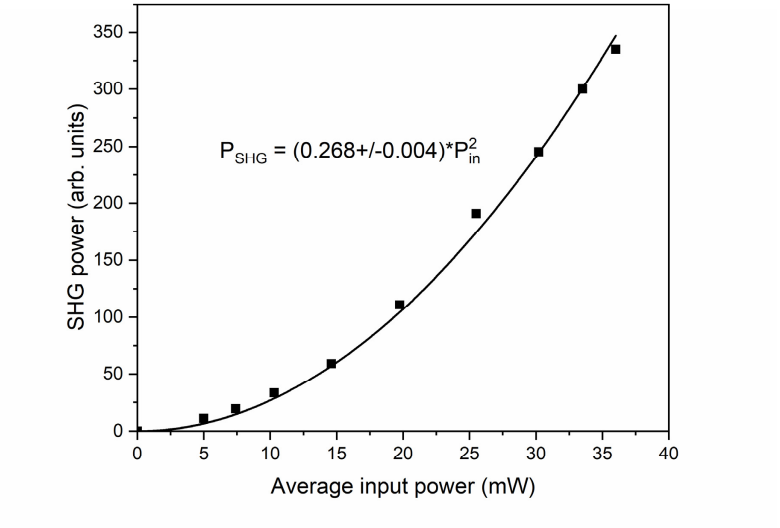

Fig. 6. SHG power generated in a 16-layer sample of Type B at 20 degrees of incidence, along with second-order polynomial fit.

3.5 Validation of the effective SON: comparison to x-cut crystalline SiO_2 (quartz)

Figure 7 shows a comparative experiment where a Type B sample with 16 layers is measured in the same conditions as a 1 mm thick, x-cut quartz sample. The pump power is reduced by a factor of 10 for the quartz in order for the SHG power to be comparable (and to avoid saturation of the detection system). Due to the bulk nature of the SON in quartz and the fact that the thickness is much larger than the phase matching coherence length of quartz (41 μm), the Maker fringes are well defined with high visibility.

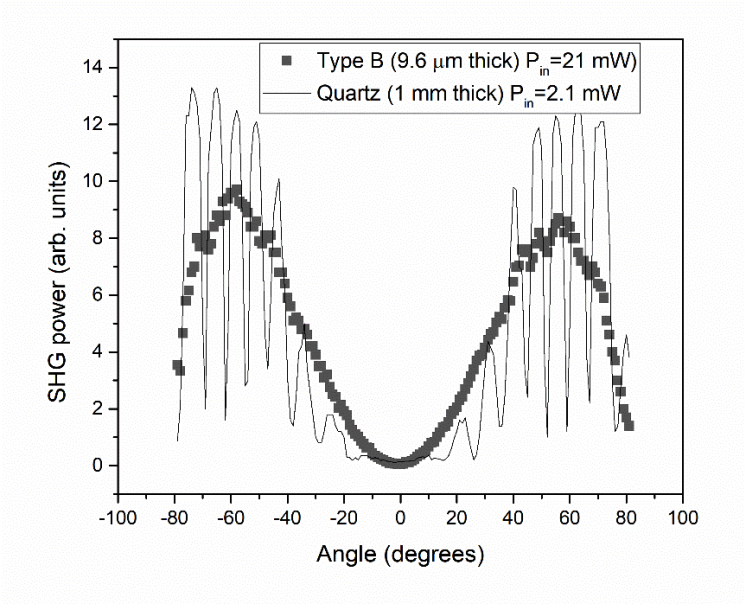

Fig. 7. Comparison of the SHG from a 16-layer Type B sample and a 1 mm thick x-cut quartz sample. The input power is decreased by a factor of 10 for the quartz sample.

Optical Materials EXPRESS

This measurement provides quantitative data from which the magnitude of the second order nonlinear coefficient d_{eff} of our samples will be estimated as follows.

At an incidence angle where the quartz result is on a peak of the Maker fringe pattern the path length in quartz is an exact odd multiple of one half of the coherence length and the sin(x) factor in Eq. (2) is equal to 1. We take the data from the angle of 48 degrees on Fig. 7. At this angle, the internal angle in the samples is 29 degrees and path lengths are longer by one over the cosine of the internal angle, i.e. 1.15 (relative to normal incidence). Taking the ratio of SHG power for the quartz and the sample at this angle (this ratio is 12/8 ± 10%) while taking into account the different pump powers used in applying Eq. (2), we get an average effective nonlinear coefficients d_{eff} across the 16 layer Type B stack of (0.03 ± 0.01) pm/V, i.e. ~one tenth that of quartz. The uncertainty is based on SHG power measurement noise and the uncertainty in the exact value of the coherence length in our samples). The nonlinearity is anisotropic and uniaxially directed perpendicular to the plane of the layers, since it was verified that there was no SHG at normal incidence and no SHG for s-polarized pump light.

4. Conclusions

The formation of an intrinsic second order nonlinear layer in a deposited stack of doped and un-doped silica glass was demonstrated. Unlike previous studies in fused silica and various other glasses, no poling was necessary to observe significant SHG from these structures. A nonlinear coefficient of 0.03 pm/V over thicknesses up to 9.6 μm was estimated from the SHG measurements by comparing to a quartz reference. The amount of SHG was observed to increase with the number of layers and total thickness, in accord with a model where the nonlinearity is due to inversion symmetry breaking at the interfaces between the layers. Annealing the samples at 800°C completely removes the nonlinear response. This indicates that quasi-phase matching would be possible in a waveguide configuration by periodic erasure of the nonlinearity with a localized heat source (such as a focused CO_2 laser beam), but not likely with intense UV irradiation, which is commonly used for thermally or optically poled samples [5,12]. The doped glass structure has a positive refractive index relative to fused silica and low linear transmission loss (the linear loss was not measurable in the UV-VIS-NIR range even in the 16 layer samples) and therefore compatible with photonic integrated circuit fabrication. However, because the nonlinearity is uniaxial, it would only be efficient for TM polarized waveguide modes (or modes with some radially polarized light in fibers).

These result also contrast with previous work on un-poled metamaterial stacks where a ternary structure (three different materials in a repeating pattern) was used to break the inversion symmetry. Since the SHG efficiency we observed increased with more spacing between the layers (Type B vs Type A, for similar thicknesses), while it increased with diminishing spacing in [27], pointing to a completely different underlying mechanism. While optimized ternary structures exhibited much larger nonlinearities (up to 5 pm/V) from an "artificially" engineered crystal-like structure, it required individual layer thicknesses of the order of 1 nm (obtained by Atomic Layer Deposition), which restricts the maximum thicknesses achievable to a few microns due to the much slower deposition rates for multilayers of that deposition technique [28]. Our results were obtained with standard PECVD deposition of binary systems of two kinds of commonly used doped silica glasses (in optical fiber and waveguide fabrication for instance), where layers with cumulative thicknesses in the tens of μm thickness are routinely feasible. The combination of test results on various layer structures point to a stress-related origin of the induced nonlinearity and further work will be required to verify this hypothesis and optimize the effect by stress engineering, should it be verified.

Funding

NSERC Strategic project grant (STPGP 463044).

Optical Materials EXPRESS

Acknowledgements

Authors would like to thank Robert Weeks, Ilya Golub, Monica Havelock, Wahab Almuhtadi, and Rebecca Trueman from Algonquin College in Ottawa for graciously allowing us access to their pulsed laser facility for the Maker fringe measurements.